Journal Name

ARTICLE TYPE

Cite this: DOI: 10.1039/xxxxxxxxxx

Multifunctional responsive fibers produced by dual liquid crystal core electrospinning†

YooMee Kye,[a] Changsoon Kim,[a] and Jan Lagerwall*[a,b]

Received Date
Accepted Date

DOI: 10.1039/xxxxxxxxxx

www.rsc.org/journalname

We demonstrate that coaxial electrospinning with more than one core channel, each containing a different type of liquid crystal, can be used to produce multifunctional fibers in a one-step process. They respond to more than one stimulus or with multiple threshold values, and the individual cores may feature different physical properties such as iridescent reflection in one core and birefringence in another. In order to ensure good fiber morphology and intact, unmixed and well separated cores, two important precautions must be taken. First, the fibers should not be collected on a hydrophilic substrate, as this will lead to severe fiber deformation and core mixing after collection, as a result of capillary forces from the water that condenses on the fiber during spinning. Second, the addition of surfactants to the polymer solution should be avoided, although it may appear beneficial for the spinning process as it reduces surface tension and increases conductivity. This is because the surfactant enters the liquid crystal core, possibly together with water in the form of inverse micelles, seriously degrading the performance of the liquid crystal.

1 Introduction

With today's surging interest in wearable and flexible technologies[1–8] there is a great need for the development of novel functional materials that combine responsiveness with softness, stretchability, light weight and convenient form factor. Such materials will play a key role in the future development of these rapidly growing research areas and they may enable a whole new range of wearable devices. Coaxial electrospinning has emerged as a promising tool for the research and development of composite fibers with the desired properties. Relying on an electric field to draw a thin jet out of a droplet of spinning solution protruding from a spinneret,[9–13] it is a low-cost, small-footprint spinning technology that is highly versatile and capable of producing core-sheath fibers that are exceptionally thin and that can carry a variety of functionalities, depending on the combination of core and sheath materials.[14–19]

For instance, the impressive range of stimulus–response relations made possible by liquid crystalline self-assembly, uniquely combining fluidity with long-range order,[20] can be introduced into fibers by coaxial electrospinning with different liquid crystals as core materials.[14] In some cases it is even possible to electrospin liquid crystal-functionalized fibers from a uniform jet, relying on solvent evaporation-induced phase separation for *in-situ* formation of the core-sheath structure.[21] A non-woven fiber mat can thus acquire e.g. the photonic crystal properties of short-pitch cholesteric liquid crystals,[20,22] exhibiting a helical structure modulation with period on the order of visible light wavelengths, that gives them striking iridescent colors. The phase transition between liquid crystal and isotropic states (the clearing point) allows the mat to function as a temperature sensor,[23] and subtle nanoscale variations in the dimensions and shape of the core channel can be revealed thanks to the confinement-sensitive structure formation.[23,24] Likewise, an ordinary nematic liquid crystal in the fiber core of a random non-woven mat can turn this into a gas sensor.[14] Very recently, the birefringence tuning of nematic liquid crystal-functionalized fibers by means of an electric field was demonstrated.[25] Importantly, there is considerable freedom to tune the morphology of electrospun fibers, the sheath being either smooth or porous and the fiber cross section being cylindrical, flat or having a more complex shape.[24,26]

A further enabling modification is the employment of multiple core flows in a single spinning jet, explored with much success by Zhao and Jiang and co-workers.[27–29] In this way three-fold coaxial fibers, with a polymer core surrounded by an intermediate liquid layer which in turn is encased by an outer polymer sheath, can be spun in a single step,[27] or several core channels can be introduced next to each other.[28,29] So far, however, each core contained the same material or, in one case, two very similar materi-

[a] *Graduate School of Convergence Science & Technology and Advanced Institutes of Convergence Technologies, Seoul National University, Suwon-si, Gyeonggi-do, Korea 443-270.*

[b] *Physics and Materials Science Research Unit, University of Luxembourg, Luxembourg, L-1523. E-mail: Jan.Lagerwall@lcsoftmatter.com*

† Electronic Supplementary Information (ESI) available: electron microscopy characterization of collapsed fibers collected on hydrophilic substrate. See DOI: 10.1039/b000000x/

als.[28] The multi-core fiber spinning concept becomes truly powerful if sufficiently different materials are encapsulated next to each other, as this would allow a single-step production of fibers with multiple functionalities and/or response capacity to multiple stimuli. For instance, the combination of liquid metal cores functioning as flexible, stretchable electrodes,[15] surrounding a liquid crystal core, might enable fibers for flexible light modulators, possibly even displays, and by combining different liquid crystals and/or different agents that adsorb at the liquid crystal–polymer interface,[30,31] high specificity in gas sensing could be ensured. While it can be difficult to avoid that a single-core fiber responds to multiple analytes, a combination of differently functionalized cores could be designed such that only the target analyte will trigger a response in all cores simultaneously. Another possibility is to use a different-colored cholesteric in each core, with different transition temperatures to the isotropic phase, for making autonomous (no need for power supply) temperature sensing fibers that give sharp responses, easily detectable optically, at multiple pre-defined temperatures.

Motivated by these stimulating perspectives we have here explored coaxial electrospinning of fibers functionalized by dual liquid crystal cores, each providing a different type of functionality and/or response. We find that this is indeed a powerful expansion of the coaxial fiber spinning concept that can enable multifunctional and highly responsive fibers, but we also identify some potential problems that must be mitigated in order to ensure success. In particular, we note that core mixing during or after spinning can be a critical problem that must be avoided in order to retain the multifunctionality of the fibers. The spinning procedure must be designed such that a sufficiently strong wall between the cores is maintained, and the fibers should not be picked up on hydrophilic substrates,[32] in order to avoid that capillary forces from water condensed on the fiber sheath during spinning induces core fluid mixing after fiber deposition. An observation of general interest is that surfactants should be avoided in the polymer sheath solution, although this is beneficial in reducing its surface tension and increasing its conductivity (and thus facilitate spinning). This is because it may diffuse into the core channels, possibly bringing with it condensed water, seriously interfering with liquid crystalline ordering.

2 Experimental

2.1 Spinneret design and components of electrospinning set-up

Several spinneret designs were explored in the search for a dual-core spinning procedure with high degree of control. For the sake of easy visual monitoring of the Taylor cone and of the core fluid flow we aimed to use exclusively transparent materials. The spinneret design used for most experiments is drawn schematically in Fig. 1 and a photo can be seen in Fig. 2a. The two core liquid crystals were pumped through two flexible silica tubes (inner diameter 100 μm) coated by polyimide (transparent but with a brown-yellow color) from BGB Analytik. In order to position these within the spinneret and prevent that they come too close to each other, they were guided through a short piece of dual-channel glass capillary (2 mm outer diameter) with θ-shaped cross section (Friedrich & Dimmock). The sheath solution was flowing through each channel of this capillary, surrounding each individual core tube. The two sheath flows merged at the end of the θ-capillary into a single Taylor cone, containing well separated core flows. Around the glass capillary was threaded a soft teflon tube with 2 mm inner diameter, much longer than the glass capillary, which was used for feeding the sheath solution. This tube was pierced in two locations upstream from the spinneret, allowing the insertion of the two core fluid tubes in one hole and a syringe needle through the other. All holes were sealed with teflon tape. The sheath solution was electrified by attaching an alligator clip from the high-voltage power supply (Gamma High Voltage) to the syringe needle. The spinneret to counter electrode distance was around 10 cm and the voltage around 10 kV. All fluids were pumped pneumatically from vials closed with septa, using a Fluigent MFCS device for rapid and accurate flow control.

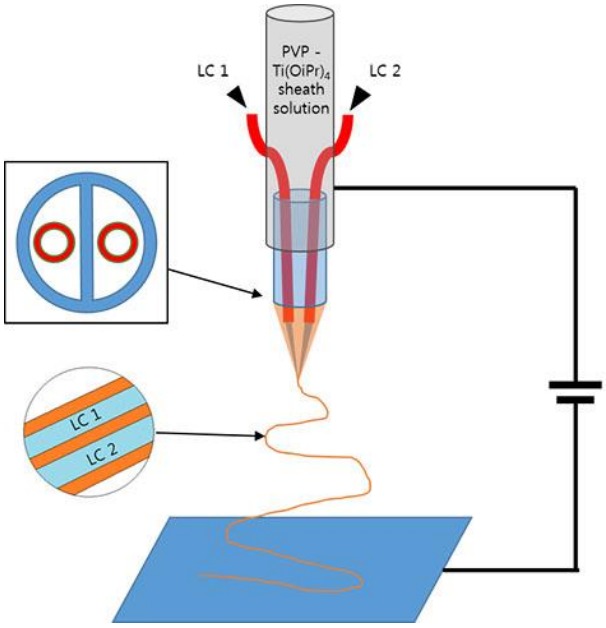

Fig. 1 Schematic drawing of the dual-core spinneret design (LC = Liquid Crystal).

2.2 Polymer solutions

The sheath solution was prepared from polyvinylpyrrolidone (PVP, molar mass 1.3 Mg mole^{-1}) in anhydrous ethanol at 18 wt% concentration. Initially, all polymer solutions additionally contained 0.5 wt% of the surfactant tetradecyltrimethylammonium bromide (14TAB) or decyltrimethylammonium bromide (10TAB), but this was left out in the final experiments. The addition of surfactant was motivated by its ability to enhance electrospinning stability through its dual function to reduce surface tension and increase conductivity.[33] To 5 mL of this stock solution was added 1.5 mL of titanium isopropoxide (Ti(O*i*Pr)$_4$ and 1 mL of acetic acid, as precursor and catalyst, respectively, for the formation of a small amount (about 9%) of TiO_2 in the sheath of the produced fibers, enhancing their mechanical stability. The

hydrolysis of TiO_2 is mediated by water condensing from the air onto the fiber jet during spinning, due to the rapid cooling of the jet as ethanol evaporates.[34].

2.3 Liquid crystals

A short-pitch cholesteric liquid crystal exhibiting red selective reflection at room temperature was prepared by mixing the multicomponent nematic mixture ROTN 615 (Roche) with the chiral dopant CB15 (Synthon Chemicals) at 65:35 ratio. In one experiment a commercial sample of ROTN 615 doped with a small amount of black dye (type and concentration not specified) was used. As non-chiral nematic liquid crystals, the single-component material 4-cyano-4'-heptylbiphenyl (5CB) and the four-component mixture E7 (both from Synthon Chemicals) were used.

2.4 Substrates for fiber collection

Fibers were collected on regular microscope glass slides, on silicon wafers, and on silicon wafers coated with a monolayer of octadecyltrichlorosilane (OTS) for hydrophobic behavior. The OTS coating was achieved either via a vapor deposition[35] or a solution immersion method.[36] For vapor deposition, silicon wafers were placed over a glass petri dish containing 300 μL OTS. The petri dish is sealed and kept in an oven at 70°C for at least 6 hours. For the solution immersion method, the silicon wafer was sequentially cleaned with acetone, isopropanol, distilled water and finally deionized water in an ultrasonic bath for 5 minutes each. The cleaned wafer was then immersed in a 1 mM OTS solution in toluene for 30 minutes. The OTS treated wafer was cleaned with toluene, acetone, isopropanol in sequence.

3 Results and discussion

3.1 Selectively reflecting and birefringent cores in a single fiber collected close to the spinneret

As a first illustration of the possibility to incorporate liquid crystals with different functionalities in one and the same fiber, we initially spun the red-reflecting cholesteric mixture in one core channel and the dye-doped nematic in the other, cf. Fig. 2. Such a combination could be useful in developing a fiber that simultaneously detects gas exposure, via its nematic core,[14] and senses tensile strain (via a color change of the cholesteric due to the shrinkage of the cross section upon fiber stretching, combined with the dependence of color on confinement[23,24]). During spinning, the shear flow unwound the helical arrangement that gives rise to the reflection color of the cholesteric, hence this mixture appears grey in the Taylor cone, as seen in the photo in panel (a) of the figure. The black dye in the other core fluid makes this easy to distinguish from the cholesteric mixture when monitoring the Taylor cone. Importantly, it allows us to confirm that no mixing of the two core phases takes place before the jet is ejected, provided optimized spinning conditions, as was the case here.

When viewing the produced fibers, deposited on a regular glass slide held into the spinning jet close to the spinneret (about 3 cm distance; the grounded electrode was placed 13 cm from the spinneret), in the polarizing microscope, we could confirm that the

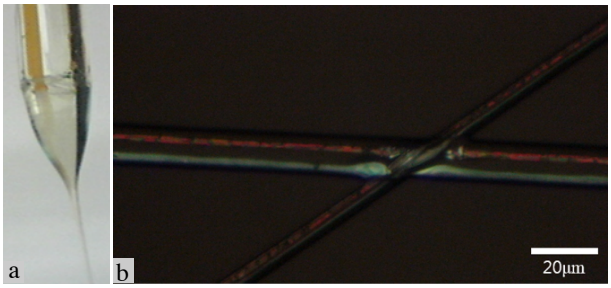

Fig. 2 (a) Photo of Taylor cone during spinning of fibers with cholesteric liquid crystal in one core and a black dye-doped nematic in the other. The flow rates were 0.4 mL hr^{-1} for the polymer solution (18 wt.-% PVP in ethanol) and 0.96 mL hr^{-1} for each liquid crystal. (b) Reflection polarizing microscopy image of the resulting fibers deposited on a glass slide, showing the red-reflecting character of the cholesteric core and the birefringence of the nematic core next to it.

cholesteric core exhibited the desired red reflection color while the other has a typical grey-white birefringence color, cf. Fig. 2b. The black dye has no impact at the single-fiber scale; only structural color, as from the cholesteric core, gives a visible impact with cores this thin. The two cores are well separated inside isolated fibers picked up at this short spinning distance and there is no clear evidence of mixing of the core fluids. However, the latter cannot be ruled out entirely because the cholesteric mixture actually contains a large fraction of the same constituents as the nematic mixture, hence a small degree of mixing would be difficult to detect. While a change in mixture composition will have an immediate effect on the color of a bulk cholesteric, the color of a cholesteric confined inside fibers of this size can to a strong degree be influenced by the cavity,[23,24] hence we cannot rely on the color as a proof of core purity.

Moreover, in locations where fibers crossed one can easily see that the fibers have merged, with serious consequences for the core integrity, indicating that the fibers were in a soft solvent-enriched state at the time of the deposition. This soft state also had the effect that the fibers largely collapsed into a flattened shape, as expected when depositing fibers on hydrophilic substrates.[32] While deposition close to the spinneret is favorable for large core and overall fiber size (desirable for maximizing the optical response from each fiber[23]), it has the disadvantage that the solvent in the polymer solution has not had sufficient time to evaporate at the time of deposition. This leads to a soft fiber sheath that allows mixing at crossing points and collapse onto the substrate. In the following we thus picked up the fibers further from the spinneret, where the sheath can be expected to be better solidified, and we also chose a different combination of liquid crystals to achieve more conclusive results.

3.2 Two nematics with different clearing points in adjacent cores.

As a means of clearly testing the integrity of the two liquid crystal fiber cores we switched to two well-known and well-characterized nematic liquid crystals, the single-component 5CB and the four-component mixture E7. Both are nematic at room temperature

but 5CB clears at 35.5°C while E7 remains nematic up to about 60°C. This considerable difference allows us to detect whether or not the two liquid crystals mixed at any point of the fiber production, by simply heating the fibers in the polarizing microscope and measuring the clearing point of each core. If any mixing of the two liquid crystals occur, we will have clearing points greater than 35.5°C and lower than 60°C for both cores, and the offset between clearing points gives an indication of how severe the mixing has been.

There was no sign of core mixing in the Taylor cone and we could indeed see dual cores in fibers deposited on regular glass slides. However, the integrity of these fibers appeared rather poor and when we heated them, the cores cleared at an intermediate temperature, only some 3-5 K apart from each other. Moreover, after cooling the fibers back to room temperature, they appeared to now have only a single core with a defect-rich nematic texture. These observations suggest that the wall separating the two cores was very fragile and that considerable core mixing had occurred at some point during the fiber production process. As shown in the ESI file we could confirm by electron microscopy that core mixing and even redistribution had taken place in a fiber produced under similar conditions, with two cholesteric mixtures as core materials.

Since the Taylor cone appearance indicated good separation of the core fluids at the onset of spinning we contemplated that the mixing actually took place primarily after fiber deposition, promoted by capillary forces acting on the outside of the fibers due to the water condensed during spinning, as it spreads on the hydrophilic substrate. This was recently demonstrated to have a major impact on the integrity and core content of coaxially electrospun fibers, with a great deal of the core fluid escaping through the fiber sheath if the deposition takes place on hydrophilic substrates.[32]

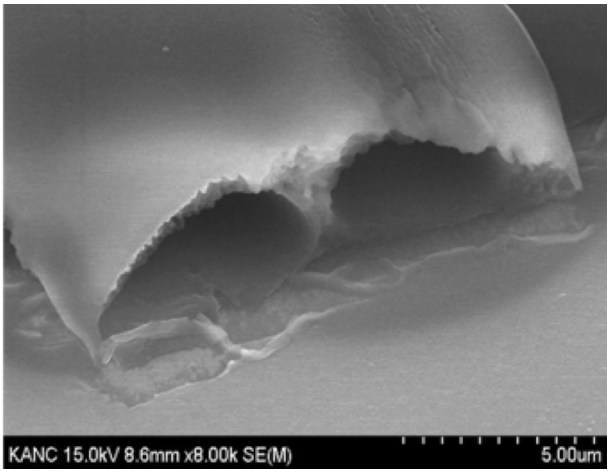

Fig. 3 Scanning Electron Microscopy image of a fractured dual-core fiber (coated with platinum for imaging purposes), with 5CB in one core and E7 in the other, deposited on a hydrophobic substrate.

We therefore switched to deposition on the hydrophobic OTS-coated substrates, resulting in a dramatic improvement of fiber quality and core integrity, as seen in the Scanning Electron Microscopy (SEM) image of the cross section of a fractured fiber in Fig. 3. It is far from trivial to fracture these soft fibers without collapse of the sheath, which in our case is thin and fully organic, in contrast to many studies of core-sheath fibers in the literature where a majority inorganic component has been incorporated and the organic polymer has been removed by calcination.[29] The resulting brittle fibers then easily fracture cleanly, allowing excellent SEM imaging of the cross section. In order to get an image of the cross section of our much more elastic fibers we first dried the fibers under ambient conditions for 24 hours in order to remove all solvent, and we then fractured the whole silicon substrate on which they had been deposited. By scoring the substrate lightly at one end and then bending it around the scored line, it fractures rapidly along a crystallographic axis of the silicon, fracturing also the fibers that cross the line of substrate fracture. In some cases the exposed cross section is sufficiently clean that an image like that in Fig. 3 can be obtained. We see that the cores are of roughly equal size and well separated, and the filling is in fact substantial, with the sheath constituting only a minor fraction of the cross section. With such a large liquid crystal filling the fiber has collapsed somewhat even on the hydrophobic substrate, yielding a hemicylindrical fiber shape.

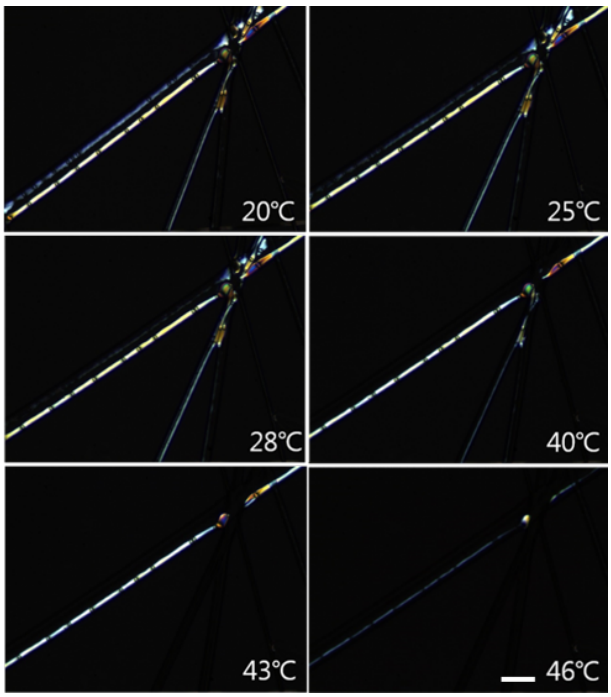

Fig. 4 Transmission polarizing microscopy images of dual-core fibers with 5CB and E7 in the two cores, deposited on a hydrophobic substrate, during heating from room temperature until both cores have entered the isotropic state. The polymer solution contained 0.5 wt.-% ionic surfactant. The scale bar is 20 μm.

When studying the nematic-isotropic transition during a heating experiment conducted on the fibers we now also noted a clear difference between the two cores, cf. Fig. 4. The 5CB core cleared at about 25°C and the E7 core at about 46°C. This difference was repeatable on heating and on cooling, with the two cores remaining intact and well separated at the end of the experiment. The

facts that the 5CB core clearing point was not intermediate between the clearing points of pure 5CB and E7, and that the two cores cleared at distinctly different temperatures, remaining intact also after cooling back to room temperature, give a clear indication that there had been no mixing between the two cores during or after spinning and that the wall separating the cores was sufficiently stable to keep the different liquid crystals separated also during heating and cooling.

While the results in Fig. 3 and Fig. 4 are strongly encouraging, as they confirm that it is possible to endow fibers with multiple levels of responsiveness via multi-core liquid crystal coaxial electrospinning, provided that the fibers are not picked up on hydrophilic substrates, we note that the clearing points of the cores, measured during the experiment in Fig. 4, are actually much too low as compared to the clearing points of pure 5CB and pure E7, respectively. It is important to note that *both* clearing points have *decreased*, ruling out mixing of the two cores as an explanation, since that would have given a decrease only of the E7 clearing point, while that of the 5CB core should have increased. We can also rule out the confinement within the fiber as the origin of the decreased clearing points, because the smooth continuous cylindrical environment provided by the electrospun fibers enhances liquid crystalline order. For thin fibers the clearing point can be considerably *increased*, for thick fibers the bulk behavior is found,[23,37,38] but a decrease in clearing point is never seen. The reason for the considerable decrease in clearing point must thus be contamination of both cores, and the cause for this can be found in the sheath solution used in these experiments.

3.3 The influence on the liquid crystal cores of surfactant in the sheath solution

To identify the source of contamination we scrutinized the composition of the sheath solution, which must either provide or facilitate the entrance of the contaminant. Eventually we realized that it does both, and that the critical component is the ionic surfactant that was added to reduce the sheath fluid surface tension and increase its electrical conductivity. The assumption was that the surfactant would end up at the sheath outside, with its hydrophilic head group towards the polar ethanol-PVP solution and its non-polar end chains directed outwards. This scenario might have been appropriate in an absolutely dry spinning atmosphere, but it is well known that under normal conditions, water from the air condenses on the fiber due to the rapid cooling as the solvent (here ethanol) evaporates. In fact, this water is a prerequisite for the hydrolysis of the $Ti(OiPr)_4$ precursor, added to the polymer solution prior to spinning, into TiO_2.[34]

In other words, water is both on the surface and within the sheath component of the jet during spinning. This means that the surfactant molecules added to the sheath solution may well migrate to the internal interface with the liquid crystal cores, where the hydrophobic end chains find an ideal environment in the liquid crystal while the polar heads are surrounded by a water-ethanol solution. Moreover, with the condensed water entering the sheath solution, the surfactant can even carry water *into* the liquid crystal core, distributed in small droplets at the centers of

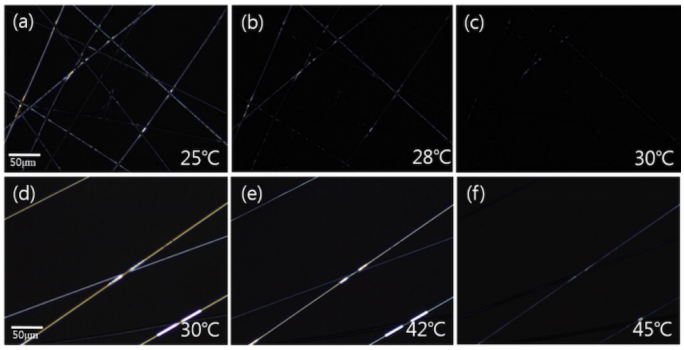

Fig. 5 Transmission polarizing microscopy images of single-core fibers with 5CB (top row) and E7 (bottom row), heated until the core turns isotropic. Both fiber series were spun with surfactant in the sheath solution.

inverse micelles that diffuse into the cores. Their small size and spherical symmetry strongly disturbs the long-range orientational order of the liquid crystal,[39] explaining why the cores clear at much lower temperature than the pure samples of each liquid crystal.

To corroborate this assumption we first spun also single-core fibers with 5CB and E7 in the core, respectively, using the same surfactant-containing sheath solution. Each of these samples exhibited clearing points close to the corresponding reduced transition temperatures seen in the dual-core fiber, about 28°C for the 5CB core fiber and about 45°C for the fiber with E7 in the core, cf. Fig. 5. Again, these transition temperatures are greatly below the well-known clearing temperatures of the pure bulk liquid crystals, in line with the expectation of surfactant and/or inverse micelles having entered also the single cores.

Finally, we spun fibers without any surfactant added to the sheath solution, in single-core format with 5CB and E7, respectively, as well as in dual-core 5CB/E7 version. When testing the clearing points in these fibers (cf. Fig. 6 and 7) they were very close to the bulk values of each pure liquid crystal, providing a final confirmation that the previous suppression of clearing points was indeed due to the surfactant in the sheath solution, most likely bringing with it condensed water in the form of inverse micelles.

4 Conclusions

We have shown that coaxial electrospinning with dual core channels containing different liquid crystals can be used to fabricate multifunctional responsive fibers in a one-step process, for instance with photonic crystal selective reflection from one core and regular birefringence in another, and with different response to temperature variation. However, in order to ensure core integrity one must first of all avoid collecting fibers on a hydrophilic substrate, because in that case post-deposition core mixing will result due to capillary forces acting from the water condensed during spinning, as it spreads away from the fiber sheath on the hydrophilic substrate. In case a hydrophobic polymer is used as sheath material, an alternative option is to spin free-hanging mats between split electrodes,[13] as the fibers are then in contact only with each other. Moreover, surfactants should not be added to

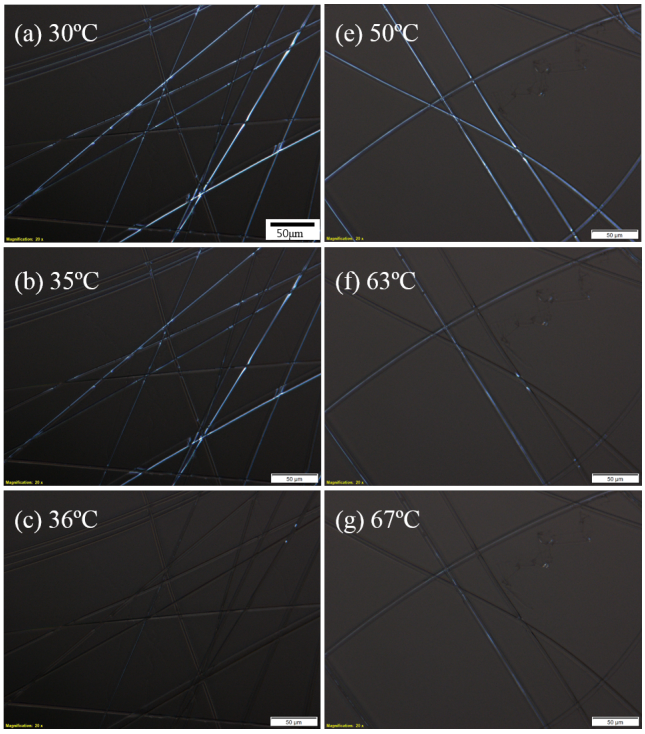

Fig. 6 Transmission polarizing microscopy images of surfactant-free single-core fibers with 5CB (left column) and E7 (right column), heated until the core turns isotropic. In contrast to the fibers spun with surfactant in the sheath solution, the clearing temperatures here correspond to the bulk clearing points of pure 5CB and E7, respectively.

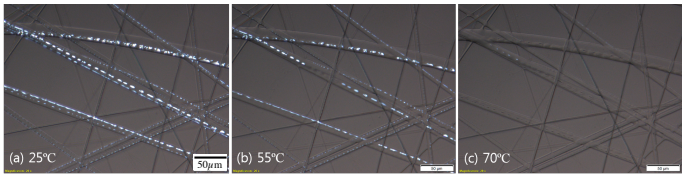

Fig. 7 Transmission polarizing microscopy images (polarizers are slightly decrossed to better visualize the fibers) of surfactant-free dual-core fibers with 5CB and E7 next to each other, heated until first the 5CB core, then the E7 core has turned isotropic.

the sheath solution when spinning fibers with liquid crystal in the core, because they enter the liquid crystal, most likely in the form of inverse micelles containing water condensed from the air during spinning, where they strongly interfere with the liquid crystal ordering process.

5 Acknowledgements

Financial support from Seoul National University (Foreign Faculty Grant 490-20110040) and from the European Research Council (Consolidator Grant INTERACT) are gratefully acknowledged.

References

1 W. Zeng, L. Shu, Q. Li, S. Chen, F. Wang and X. Tao, *Adv. Mater.*, 2014, **26**, 5310–5336.
2 L. Kou, T. Huang, B. Zheng, Y. Han, X. Zhao, K. Gopalsamy, H. Sun and C. Gao, *Nat. Commun.*, 2014, **5**, 3754.
3 S. Patel, H. Park, P. Bonato, L. Chan and M. Rodgers, *J. Neuroeng. Rehab.*, 2012, **9**, 21.
4 P. Bonato, *IEEE Eng Med Biol Mag*, 2010, **29**, 25–36.
5 S. Cheng and Z. Wu, *Lab Chip*, 2010, **10**, 3227–3234.
6 D.-H. Kim and J. A. Rogers, *Adv. Mater.*, 2008, **20**, 4887–4892.
7 B. Shim, W. Chen, C. Doty, C. Xu and N. Kotov, *Nano. Lett.*, 2008, **8**, 4151–4157.
8 F. Axisa, P. Schmitt, C. Gehin, G. Delhomme, E. McAdams and A. Dittmar, *IEEE Trans. Inform. Technol. Biomed.*, 2005, **9**, 325–336.
9 X. Lu, C. Wang and Y. Wei, *Small*, 2009, **5**, 2349–2370.
10 D. Reneker and A. Yarin, *Polymer*, 2008, **49**, 2387–2425.
11 G. Rutledge and S. Fridrikh, *Adv. Drug Delivery Rev.*, 2007, **59**, 1384–1391.
12 A. Greiner and J. Wendorff, *Angew. Chem. (Int. Ed.)*, 2007, **46**, 5670–5703.
13 W. Teo and S. Ramakrishna, *Nanotechnology*, 2006, **17**, R89–R106.
14 D. K. Kim, M. Hwang and J. P. F. Lagerwall, *J. Polym. Sci. B Polym. Phys.*, 2013, **51**, 855–867.
15 H. Yang, C. Lightner and L. Dong, *ACS Nano*, 2012, **6**, 622–628.
16 A. L. Medina-Castillo, J. F. Fernández-Sánchez and A. Fernández-Gutiérez, *Adv. Funct. Mater.*, 2011, **21**, 3488–3495.
17 E. Zussman, *Polym. Adv. Technol.*, 2011, **22**, 366–371.
18 A. Yarin, *Polym. Adv. Technol.*, 2011, **22**, 310–317.
19 J. McCann, M. Marquez and Y. Xia, *Nano. Lett.*, 2006, **6**, 2868–2872.
20 P.-G. de Gennes and J. Prost, *The Physics of Liquid Crystals*, Clarendon Press, Oxford, UK, 1993.
21 A. Buyuktanir, Ebru, W. Frey, Margaret and L. West, John, *Polymer*, 2010, **51**, 4823–4830.
22 J. P. F. Lagerwall and G. Scalia, *Curr. Appl. Phys.*, 2012, **12**, 1387–1412.
23 E. Enz and J. Lagerwall, *J. Mater. Chem.*, 2010, **20**, 6866–6872.
24 E. Enz, V. La Ferrara and G. Scalia, *ACS Nano*, 2013, **7**, 6627–6635.
25 J. Wang, A. Jákli and J. West, *ChemPhysChem*, 2015.
26 G. Scalia, E. Enz, O. Calò, D. K. Kim, M. Hwang, J. H. Lee and J. P. F. Lagerwall, *Macromol. Mater. Eng.*, 2013, **298**, 583–589.
27 H. Chen, N. Wang, J. Di, Y. Zhao, Y. Song and L. Jiang, *Langmuir*, 2010, **26**, 11291–11296.
28 N. Wang, H. Chen, L. Lin, Y. Zhao, X. Cao, Y. Song and L. Jiang, *Macromol Rapid Comm*, 2010, **31**, 1622–1627.
29 Y. Zhao, X. Cao and L. Jiang, *J. Am. Chem. Soc.*, 2007, **129**, 764–765.
30 S. Sridharamurthy, K. Cadwell, N. Abbott and H. Jiang, *Smart Mater. Struct.*, 2008, **17**, 012001.
31 G. Lee, F. Araoka, K. Ishikawa, Y. Momoi, O. Haba, K. Yonetake and H. Takezoe, *Particle & Particle Systems Characterization*, 2013, **30**, 847–852.
32 D. K. Kim and J. P. F. Lagerwall, *ACS Appl. Mater. Interf.*, 2014,

6, 16441–16447.
33 T. Lin, H. Wang, H. Wang and X. Wang, *Nanotechnology*, 2004, **15**, 1375.
34 D. Li and Y. Xia, *Nano. Lett.*, 2003, **3**, 555–560.
35 C. Saner, K. Lusker, Z. Lejeune, W. Serem and J. Garno, *Beilstein J Nanotechnol*, 2012, **3**, 114–122.
36 Y. W. Yi, H. G. Robinson, S. Knappe, J. E. Maclennan, C. D. Jones, C. Zhu, N. A. Clark and J. Kitching, *J. Appl. Phys.*, 2008, **104**, 023534.
37 E. Enz, U. Baumeister and J. Lagerwall, *Beilstein J. Org. Chem.*, 2009, **5**, DOI: 10.3762/bjoc.5.58.
38 J. P. F. Lagerwall, J. T. McCann, E. Formo, G. Scalia and Y. Xia, *Chem. Commun.*, 2008, **42**, 5420–5422.
39 J. Yamamoto and H. Tanaka, *Nature*, 2001, **409**, 321–325.